Automatika

Journal for Control, Measurement, Electronics, Computing and Communications

ISSN: (Print) (Online) Journal homepage: https://www.tandfonline.com/loi/taut20

A novel centralized supervisory with distributed control system-based microgrid

T. Srikanth & S. Chitra Selvi

To cite this article: T. Srikanth & S. Chitra Selvi (2022) A novel centralized supervisory with distributed control system-based microgrid, Automatika, 63:3, 482-495, DOI: 10.1080/00051144.2022.2052663

To link to this article: https://doi.org/10.1080/00051144.2022.2052663

Published online: 21 Mar 2022.

AUTOMATIKA
2022, VOL. 63, NO. 3, 482–495
https://doi.org/10.1080/00051144.2022.2052663

A novel centralized supervisory with distributed control system-based microgrid

T. Srikanth and S. Chitra Selvi

Department of Electrical and Electronics Engineering, Anna University - University College of Engineering, Nagapattinam, India

ABSTRACT

Supervisory Control and Data Acquisition is a popular control and monitoring scheme and is predominantly used in many industrial systems. Driven by the motivation of extending the usage of the SCADA systems for microgrid, a novel centralized Supervisory Control and Data Acquisition System with Distributed Control Systems is proposed and validated for the microgrid. Supervisory instructions are issued from the central control system, whereas the local controllers are used to implement the exclusive control schemes required for the various subsystems. A wired sensor network is used to monitor the various vital parameters and a Graphical User Interface (GUI) is used for monitoring the status of operation of the various subsystems along with their parametric values. The proposed system is simulated in the MATLAB SIMULINK environment. An experimental verification prototype has also been carried out where a PC (Personal Computer) with a Graphical User Interface developed in C# and a microcontroller is used to act as an interface between the distributed controllers in the plant and the master control PC.

ARTICLE HISTORY
Received 4 October 2021
Accepted 7 March 2022

KEYWORDS
SCADA (Supervisory Control and Data Acquisition System); DCS (Distributed control system); GUI (Graphical User Interface); energy management; MPPT (Maximum Power Point Technique); SMC (Sliding Mode Controller)

1. Introduction

A microgrid is a miniature power system consisting of a number of power sources brought to a common pool shared by several loads [1]. Some of the sources may be derived from renewable energy resources and may be of different electrical forms like different voltage levels, AC or DC and so on. Similarly, the loads attached to the microgrid may require electrical power in diversified forms like DC or AC single phase, three phase, different voltage levels and so on. The special feature of the microgrid is that all the loads connected to the microgrid get the appropriate magnitude and form of power and that there is a provision for converting the diversified forms of power available to diversified forms of requirements [2].

Power electronic converters play an important role in the conversion of power from one form to the other. Depending upon the form of the available sources and the specific requirements of the loads to be served, several power electronic converters are used [3]. The presence of a large number of sources and loads operating with different voltage levels, power and so on makes the control requirements of the microgrid much complex [4].

There are many parameters to be monitored, and many to be controlled. The whole control systems are to be built on some complex decision-making algorithms. The microgrid therefore needs an efficient and automated Supervisory Control and Data Acquisition (SCADA) systems. SCADA and Distributed Control Systems are well-established control schemes used in the industries. Microgrids and their applications have received keen attention by many researchers [5–7]. In addition to advanced control systems, the suitable Pulse Width Modulation schemes are also required in the development of the microgrid. The other direction of research has been the development of PWM (Pulse width modulation) pulses that ultimately lead to an improved quality of power delivered to the load [8]. The PWM techniques influence the power quality of the voltage or current produced by the inverters.

There are many research contributions recorded in the literature in the field of developing various advanced PWM systems [9–14]. With the advent of modern digital computer and the advanced software tools, it has become possible to develop complex systems in short periods. Fuzzy Logic Control, the ANN (Artificial Neural Networks)-based control and the ANFIS (Artificial Neuro fuzzy inference system)-based control schemes are all useful control algorithms [15,16]. Many authors have contributed a lot of technical developments using these techniques. Optimization is another scheme of selection of operational parameters like the constants of the PI controller, etc. that has also been exploited by a number of researchers [17–20].

CONTACT T. Srikanth sriphd92@gmail.com Department of Electrical and Electronics Engineering, Anna University- University College of Engineering, Thirukkuvalai, Nagapattinam 610204, India

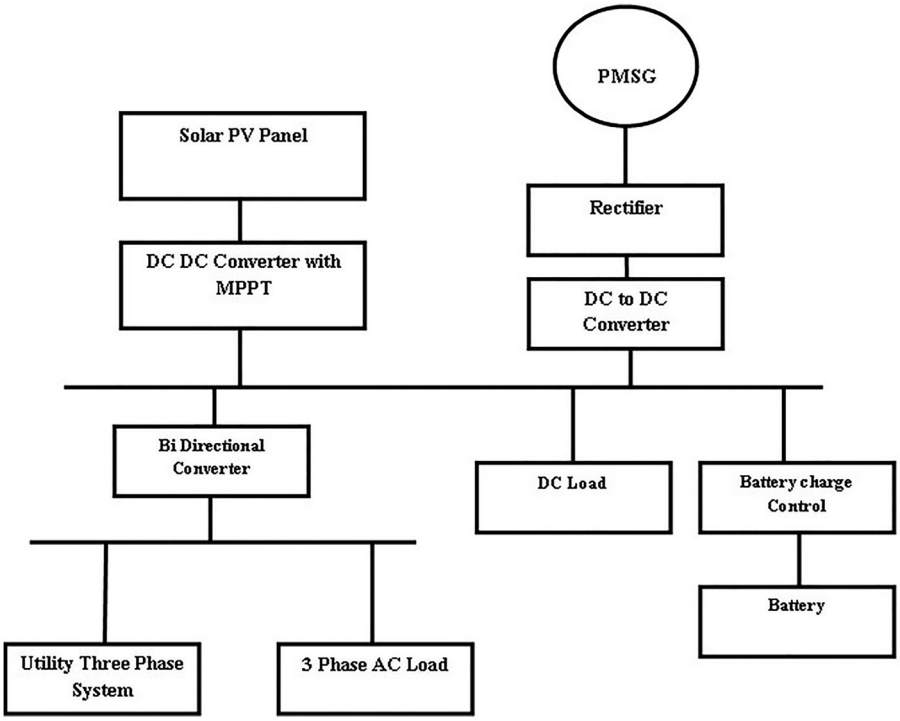

Figure 1. Block Schematic of the proposed system.

The Supervisory Control and Data Acquisitions (SCADA) and the Distributed Control Systems (DCS) play important role in the process and production industries [21–24]. The motivation behind this work is to make use of the benefits of SCADA and DCS to be utilized in the management of the microgrid systems.

In this work, the implementation of the SCADA and the DCS systems for microgrid is demonstrated. The proposed system also indicates a battery-based storage system. The block diagram of the proposed work is shown in Figure 1. The power flow analysis among the various subsystems could be centrally monitored. The central control system is implemented in a computer. The complete plant data can be communicated to this computer. In the industrial environment manner many such independent or inter-dependent microgrids can be governed by a common computer.

The paper has been arranged as follows. Following this brief introduction,

Section 2 outlines the various subsystems used in this system.

Section 3 presents the modelling of the proposed system in the MATLAB and the results of simulations have been presented in this paper.

Section 4 explains the details of the experimental prototype that has been developed. The implementation of various control schemes using the embedded control systems for individual power conversion systems and the details of the master control scheme and the PC-based GUI are also explained in this chapter. In Section 5, important observations in the simulations and the experimental verifications are presented followed by the conclusion and reference sections.

2. Proposed system

2.1. Subsystems of the proposed system

The following subsystems are connected to the microgrid.

1. Solar PV-based DC-to-DC converter.
2. Wind turbine driven PMSG.
3. Battery system.
4. Grid connected bidirectional AC/DC converter.
5. AC three-phase load.
6. DC load.

The solar PV system delivers power in the DC form to the DC bus bar. The DC load is also connected to the DC bus bar through a DC-to-DC converter. The wind energy harvesting system supplies three-phase AC power into the three-phase AC bus bar. The power ratings of each of the subsystems are tabulated and given in Table 1.

There are different modes of operation possible with the proposed microgrid system. The various modes

Table 1. System parameters.

System	Nominal operating voltage	Nominal power rating
Solar PV source	120 V	1000 W
Wind source	Three phase 380 V 50 Hz	2500 W
DC load	200 V	4000 W
Battery	360 V	3000 Ah
Bidirectional Converter AC/DC	400 V DC/380 V AC 50 Hz	10000 W
AC load	Three phase 380 V 50 Hz	3 kW 3 kvar

Table 2. Modes of operation.

System	Bit	1	0
Solar PV source	B0	Available	Not available
Wind source	B1	Available	Not available
Auxiliary DC source	B2	Available	Not available
DC load	B3	On	Off.
Battery	B4	Charging	Discharging
Bidirectional Converter AC/DC	B5	DC-to-AC	AC-to-DC
AC load	B6	On	Off
Configuration	B7	Grid	Stand alone

Table 3. Mode code configuration.

Mode	Configuration	System ON	System OFF	Mode Code
Mode 1	Stand Alone	PV, WG, Aux.DC, DCL, Bat. BDC, ACL, Config.	Utility	01111011
2	Stand Alone	PV, Bat, DCL	Utility, WG, Aux. DCL, ACL	0011001
3	Grid Integrated	PV, WG BDC, Aux DC, BDC	DCL ACL BAT	0100111
4	Grid Connected	ACL DCL BDC	PV, WG, Aux. DC Bat	1101000

of operation possible with the proposed system are tabulated and shown in Table 2. The different modes of operation are binary codified and position of the individual subsystems in the data string are shown in Table 2.

Systems that are ON are assigned status 1 and those OFF are assigned 0. For example, the data string 110101011 gives the following information: Solar PV ON; Wind ON; Aux. DC Source OFF; DC load OFF; Battery Charging; Bidirectional Converter ON; AC load ON – (BDC) Grid Connected ON.

Mode 1: The different source that are available are the PV source, the WG Source and the Aux. DC source. The loads that are operational are the DCL and the ACL. There is no power export or import with the grid.

Mode 2: The only source available is from the PV subsystem. The only load is also the DC load. There is no power export to the grid. The battery is used to store the excess of renewable energy.

Mode 3: The different sources that are available are the PV source, the WG Source and the Aux. DC source. Both the DC load and the AC load are not operated. Hence the power harvested is totally exported to the grid. In this mode of operation, the bidirectional converter is operational and the power harvested is integrated into the grid through bidirectional power converter.

Mode 4: The renewable energy sources are not available. However, the ACL and the DCL demand power. Hence, the bidirectional convertor import power from the utility source and the demands at the load are met with. Similar to the data set shown in Table 3 many combinations of sources and loads can be included or excluded and accordingly the data bits are generated. Thus, many modes are formed. In this work, the eight-bit data word is logged into the master control PC through the microcontrollers near the PC. Between the plant and the microcontroller, the data link is in the parallel form. Between the PC and the microcontroller, the data link is serial. Based on the values of the vital parameters, the availability of the renewable sources and the demand the modes are determined either manually or automatically by the master controller and the status indicated in the GUI on the master control computer.

Table 4. PV parameters.

Parameter	Value
Open circuit Voltage	22.2 V
Short circuit Current	5.45 A
Voltage at P_{max}	17.2 V
Current at P_{max}	4.95 A

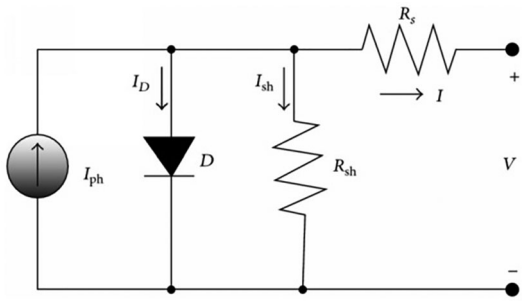

Figure 2. The diode model of the PV cell.

2.2. Solar photo voltaic source

The PV source is derived from a solar PV farm of power capacity 4 kW. The base voltage of the solar farm is 120 V and it is stepped up to the required 400 V DC level by a generic Buck Boost Converter. The details of the solar farm are shown in Table 4.

$$Ipv - Io[\exp\{\propto KT\} - 1] - \frac{V + IRs}{Rsh}. \qquad (1)$$

A set of 8 PV panels of rating given in Table 4 are connected in series to form a string and a set of 6 strings are used. The maximum power rating of each panel is 85 W. The total power rating of the solar PV farm is $85 * 48 = 4080$ W. The rated output voltage of the PV farm is $17.2 * 8 = 137.6$ V. The DC bus bar voltage is 400 V. A DC-to-DC generic boost converter is used in between the PV farm and the DC bus bar.

The circuit arrangement of the PV cell is shown in Figure 2. The specification of the components used for the buck boost converter is shown in Table 5.

2.3. Wind energy conversion system using a PMSG

The system includes a Wind Energy Conversion System (WECS). The WECS uses a three-bladed horizontal type wind turbine. It is coupled to a PMSG (Permanent magnet synchronous generator). The PMSG is a

Table 5. Buck boost converter specifications.

Parameter	Values
Nominal V_{in}	120 V
V_{out}	400 V
Power rating	5000 W
Switching frequency 20 kHz	
MPPT	Sliding Mode Controller (SMC)
Inductance L	1 mH
Capacitor C	2200 mF

20kHz value comes in column section.

Table 6. Wind energy systems rating.

Parameters	Value
Wind turbine	
Type horizontal	9 m/s
Nominal wind velocity	2.5 kW
Nominal power rating	
Generator	
Type	PMSG
No. of phases	3
Power rating	2.5 KVA
Maximum speed	4000 RPM
Rectifier	
Type	Diode bridge 6 pulse rectifier
Voltage	100 V
Current	50 A
Power	
Boost converter	
Type	Generic boost converter
Vin	100 V
Vout	500 V
Power rating	5000 W

three-phase AC generator with variable frequency output. The output frequency of the three-phase AC output of the PMSG is a function of the speed of the shaft and the number of poles. The wind turbine runs at a slower speed and the system uses a gear box. The PMSG may also be run at slow speed in which case the PMSG with larger number of magnetic pole pairs are used so that the frequency of the AC output is high even though the shaft speed is low.

The PMSG-based wind energy conversion system belongs to the variable speed WECS category. Maximum Power Point Tracking is used in this variable speed WECS. The three-phase AC output of the PMSG, being a variable frequency AC source, cannot be either grid integrated directly or is suitable for three-phase or single-phase AC loads which require fixed 50 HZ supply.

The variable frequency AC output of the PMSG is therefore rectified into DC by a Diode Bridge Rectifier (DBR). The DBR is a rectifier with no control degree of freedom. The output of the rectifier is fed as input to a DC-to-DC boost converter. The boost converter makes the output voltage equal to the common DC bus bar voltage while it includes the MPPT control as well. The specifications of the WECS are given in Table 6.

There is a battery connected across the DC bus bar through the battery charge control system which uses a bi-directional buck boost converter. The battery is being charged by the DC bus. When the wind, solar and the utility power supply all fail, the battery is meant

Table 7. Three phase load specifications.

Parameter	Specification
Type of load	3 phase RL load
Voltage	380 V LL
Frequency	50 Hz
Power rating real power	5 kW/Phase
Reactive power	5 kvar/Phase

to supply the critical loads including the control systems. There are separate DCS units responsible for the MPPT of the WECS, the control of the boost DC-to-DC converter. Wind velocity, the power delivered to the DC link, the DC link voltage, the SOC of the battery and the terminal voltage across the three phase inverter nodes are monitored by the SCADA. The supervisory controller can include or exclude the WECS, the battery system and the three-phase inverter in the WECS.

2.4. AC three-phase load

There is a three-phase AC load with variable real and reactive power demands. The line voltage of the AC bus bar is 380 V and it is maintained at a frequency of 50 Hz. The two sources of AC power are the utility source and the bidirectional power converter.

When the three-phase utility fails, this AC three-phase load can be driven by making use of the DC power derived from the DC sources and routed to the three-phase AC bus bar through the bidirectional DC/AC converter. There is no local controller in association with this load; however, there is a provision to disconnect or connect this load to the three-phase AC bus bar from the central SCADA unit. The ratings of the three phase load are given in Table 7.

2.5. DC load

The microgrid supports DC as well as AC loads. The DC load connected to the microgrid is a 4000 W resistive load. The operating voltage of the DC load is 200 V. The DC load is powered from the DC bus bar. There is a buck converter in between the 400 V DC bus bar and the load terminals. The buck converter is provided with a control system that regulates the voltage across the load at 200 V.

The DC load can be turned ON or OFF by the central control system as well. The voltage regulation system is embedded in a local microcontroller placed close to the buck converter.

2.6. Bi-directional AC/DC converter

The component that links the AC and the DC bus bars is the bidirectional power converter. The standard Graetz bridge converter is used for this purpose. The Graetz bridge converter has a three-phase AC side and a DC side. The DC side is connected across the DC bus bar.

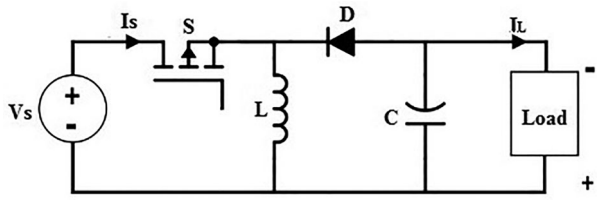

Figure 3. The buck boost converter.

The AC side of this converter is connected across the three-phase AC bus bar through a set of three RL filter units.

The Graetz bridge converter is a three leg six pulse converter. It has a set of DC rails and three legs with two power electronic switches in each leg. The junction of the two power electronic switches in each leg is known as a node and thus there are three nodes. These three nodes are connected to the AC bus bar through a passive filter section.

The bidirectional converter can draw power from the AC bus bar and transfer it to the DC bus bar. It can work in the reverse direction also. Depending upon the direction and the magnitude of power transaction, real or reactive, a suitable three-phase reference signal is generated and this reference signal is used in a sinusoidal PWM section to generate the switching pulses. The master controller or the SCADA system directly controls this bidirectional power transaction system.

2.7. Solar photo voltaic system

The equivalent circuit and the equation for output current of the PV cell are shown in Figure 3 and Equation 1, respectively [2]. The relationship between the terminal voltage across the PV panel and the output current of the PV panel is nonlinear. The VI characteristic and the PV characteristic of a typical solar cell are different for different solar insolation levels.

On the PV characteristics there exists a unique point which corresponds to the maximum power delivered to the load. This occurs only when the panel voltage is maintained at a certain specific level. For different solar insolation levels, the maximum power that could be harvested and the corresponding terminal voltage of the PV panel are different.

2.8. MPPT for the solar photo voltaic system

The maximum power rating of the solar farm is 1 kW. It is expected that the solar insolation levels change unpredictably in a random manner. It is also assumed that the entire PV panel experiences the same solar irradiation and temperature and there is no partial shading. As such, depending upon the solar insolation a fast-acting MPPT is required so that the harvested power is maximum at all solar insolation and temperature levels. The SMC method of the MPPT is used for the solar PV system.

2.9. MPPT for the wind energy subsystem

The power extracted from the PMSG is maximum if and only if the wind turbine that drives the PMSG is driven at the specific speeds for the different wind

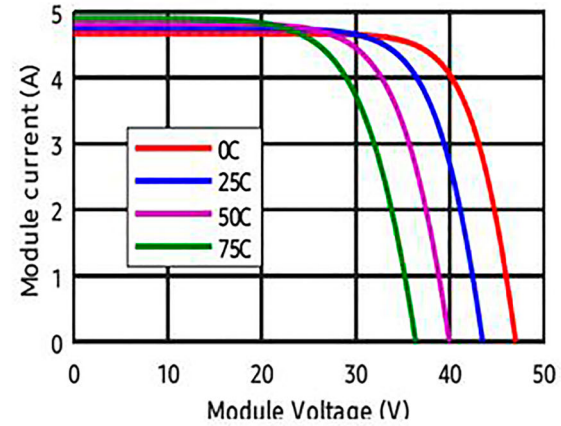

(a)

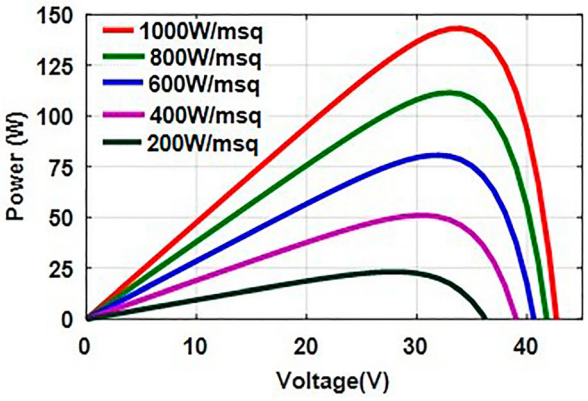

(b)

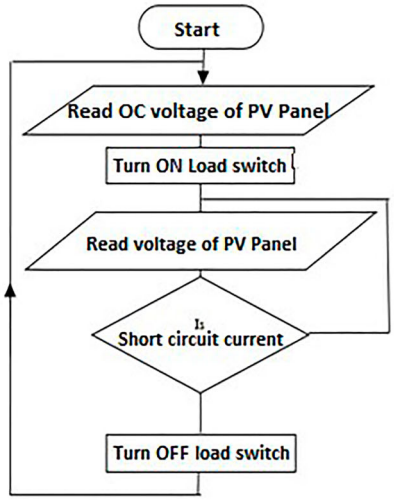

(c). The flow chart of the SMC type MPPT

Figure 4. PV Panel Characteristics: (a) I–V Characteristics. (b) P–V Characteristics. (c) The flow chart of the SMC type MPPT.

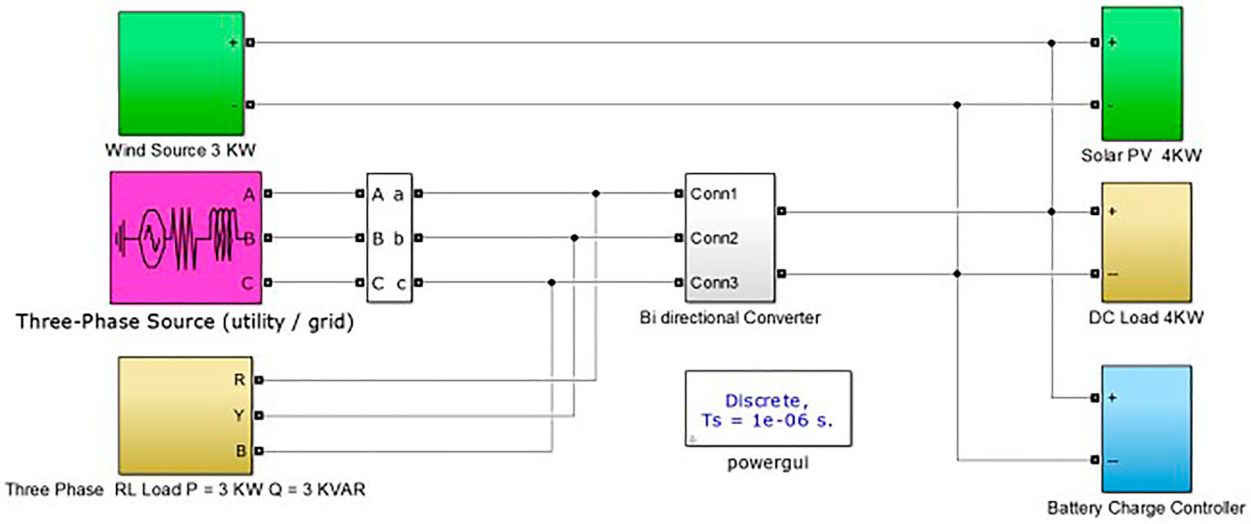

Figure 5. SIMULINK Subsystems: The MATLAB SIMULINK model of the proposed system.

velocities. For any given wind velocity, it is possible that the wind turbine is run at different speeds by controlling the pitch angle of the blades or by controlling the electrical load on the generator.

3. Simulations in the MATLAB SIMULINK

3.1. SPV energy conversion subsystem

The specifications of the solar farm and the specifications of the components used in the associated DC-to-DC boost converter are given in Table 5. In this section, the complete modelling in the MATLAB SIMULINK is presented. The various subsystems include the solar PV subsystem, the WECS subsystem, the three-phase load, the DC load, the bidirectional converter and the three-phase utility outlet. PV panel characteristics and the flow chart of SMC type MPPT are shown in Figure 4.

The solar PV system includes the solar PV unit and a boost converter. The MPPT is achieved using a SMC implemented in the boost converter. The buck boost stage also has a control system to regulate the terminal voltage at 400 V DC along with a current limiting scheme, respectively.

Depending upon the solar insolation, the power harvested vary and the harvested power is pumped into the DC bus bar in the fixed voltage variable current method. Whenever the solar insolation changes, the current fed into the DC bus bar changes. The solar power system has a set of two DC-to-DC converters. Although it is possible to boost the available DC input voltage of 120 V to 400 V in a single stage, it has been preferred to use a two-stage boost operation so that the boost converters, in cascade may operate at lower duty cycles and that they avoid operating in the steep nonlinear region of operation of the boost converter.

A battery subsystem is also included in this work. The purpose of the battery is to deliver power to

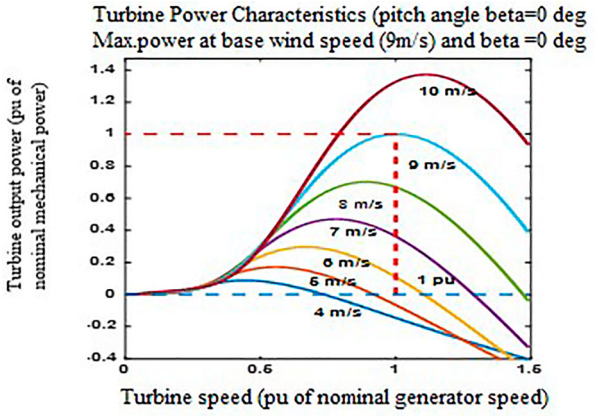

Figure 6. The family of characteristic curves.

the critical loads like the instrumentation systems in the absence of the solar wind and the utility systems. The battery is essential to maintain communication between the nodes and the master controller so that the presence or absences of the renewable sources is updated so as to make control decisions.

The buck converter is active when the renewable or the utility sources are available so that the battery is charged. The battery supports the DC bus bar of 400 V when the renewable and the utility sources fail Figure 4.

The electrical load on the PMSG is controlled by manipulating the duty cycle used by the boost converters used in the power conversion chain. The MATLAB SIMULINK subsystems has shown in Figure 5. In this work, the Perturb and Observe algorithm is used by monitoring the DC power output and the PWM duty cycle is adjusted until the electrical power harvested as monitored across the DC link in the power converter chain of the PMSG Figure 5.

The family of curves relating wind velocity, the turbine speed and the electrical power harvested for various wind velocities is shown in Figure 6.

Table 8. Power balance for scenario 1.

Source/Load	Magnitude
Wind	2.2 kW
Solar	1.1 kW
Total Demand	2.7 kW
To Battery	0.6 kW

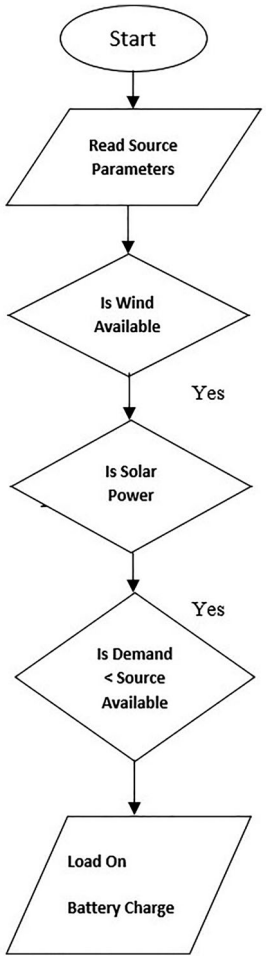

Figure 7. Flow chart for Scenario 1.

The following three scenarios were studied in the simulation,

3.2. Power balance

The main sources of power are the PMSG-based wind energy source, the solar power source and the utility source. The capacity of the wind and the solar power sources is given in Table 8. There is a battery backup available to be used in case failure of all sources. The battery backup is primarily meant for supplying the instrumentation systems that is considered critical.

The maximum total load is 5 kW. There are different scenarios of operations. The different scenarios arise by the inclusion and exclusion of different loads and sources. The renewable energy sources that depend mainly on the environmental conditions cannot provide output power consistently, depending upon the wind velocity the power output of the wind turbine gets changed and similarly depending upon the solar insolation and the ambient temperature the power output of the solar farm also gets changed. The magnitude of power production by the renewable energy systems is quite unpredictable and many scenarios arise.

Table 9. Power balance for scenario 2.

Source/Load	Magnitude
Wind	1.2 kW
Solar	0.8 kW
Total demand	2.7 kW
Utility	0.7 kW

Table 10. Power balance for scenario 3.

Source/Load	Magnitude
Wind	0 kW
Solar	0 kW
Utility	0 kW
Critical load	0.4 kW
From battery	0.4 kW

3.2.1. Scenario 1

The wind and solar power are fully available. The load on the grid is less than the total generation. The excess energy generated by us either routed to the battery or to the utility grid. A flow chart may be developed for this scenario and is shown in Figure 7. The power balance under this scenario is shown in Table 8.

3.2.2. Scenario 2

The wind and the solar sources are available partially and even when combined they cannot meet the load requirements. The battery is either full or of partial SOC. When the wind and solar power sources are partially available, the utility source also supports the load. The battery is not used now. If the battery SOC is below a critical value, then it is charged from the utility source.

The total power demand is now shared by the utility along with the partially available renewable sources as shown in Table 9.

3.2.3. Scenario 3

The conditions of the third scenario are given in Table 10. In this scenario, neither the renewable energy source nor the utility is available. The battery is supplying only the critical load.

We studied the performance of a power balance depend on the P–Q Control scheme under different operating conditions that the modernized inverters can deliver. According to the achieved results, the inspected P–Q regulation scheme supplies exact and rapid management of active and reactive power vaccinated to the grid and furnished from the PV array. Additionally, inspected harmonic spectra of injected active and reactive power, PV Voltage, DC link voltage and current verify that the proposed control scheme ensures the activity at high power quality.

4. Experimental setup

4.1. Power converters for microgrid system

The following power electronic converters were used in the prototype of the microgrid that has been used to validate the proposed ideas.

a. The boost converter for the SPV system.
b. The buck converter to charge the battery.
c. The boost converter for the fuel cell.
d. The diode bridge rectifier for the PMSG.
e. The boost converter for the PMSG.
f. The three-phase inverter for the PMSG.
g. The bidirectional DC/AC converter.

The system parameters used in the boost converters were the same. All the boost converters used in the system are identical so that they can be used interchangeably among all boost converter units. The specifications of the boost converters are the same as used in the simulation. The inherent resistance of the inductor and the equivalent series resistance of the capacitors are ignored. The switching frequency was 5 kHz. The DC bus voltage has been maintained as 48 V and the batteries are of a nominal 12 V range.

4.2. Master and local control schemes

The overall system can be viewed as the combination of a number of local control systems and the master control system. The master control system takes care of the energy management. The local controllers are associated with the individual converters and they take care of MPPT for renewable sources and local voltage regulation systems. The master controller is embedded with the master computer. The local control schemes are built around the individual microcontrollers. The master controller is built in the PC with a GUI. The GUI gives the information of all operational parametric values and the modes of operation. The user can override the modes of operations through the GUI. The GUI on the master computer is programmed in C#. The master controller gets all relevant data through a microcontroller on the PC side. The PC side microcontroller interfaces the subsystems and the master control PC.

4.3. Data collection system

The microgrid system and the proposed SCADA-based management system needs a number of physical parameters to be monitored by the local controllers and the master controller. All the vital parameters are monitored by the master controller. The master controller needs this information because it is responsible for the overall management of the microgrid including power transaction. All the vital parameters are brought to the main microcontroller. Power flow and control scheme waveforms are shown in Figure 8. The main microcontroller converts them all into equivalent digital data and the data are logged into the master control PC through the USB (Universal synchronous bus) interface. The output of the main microcontroller is sent out through the serial port of type RS232 and this data are converted to be suitable to the USB form by a RS232 to USB converter. Since the responsibility of the master controller is power routing, only the vital parameters that are required for decision-making regarding the flow of power are to be logged on to the master controller.

In case of renewable energy systems and the battery, the terminal voltage and the output current are required to monitor their power output. Eight parameters are logged into the master controller. The eight parameters monitored are the PV panel terminal voltage, the PV current, the fuel cell voltage and current, the three phase voltage across the AC bus bar, the three phase AC load current and the terminal voltage across the output of the boost converter used for the wind power conversion chain.

A number of PIC (Programmable interface controllers) microcontrollers 16F877A are used. In association with each source or load, a PIC is used. These controllers are used as local controllers that are used to make local decisions like voltage regulation, current limitation and maximum power point tracking. These controllers do not have any control over other converters in the network than the one they are exclusively meant for Figure 8.

Each PIC 16F88777A controller has a couple of PWM outputs and 8 analogue input channels. The switching frequency used in a power converter can be changed by changing the PWM frequency. Both of the two PWM channels should be of the same frequency. However, they may operate under different duty cycles. The voltage regulation and MPPT activities are carried out by employing the analogue inputs and the PWM outputs.

The prototype developed, as shown in Figure 9, is a scaled down version of the model proposed and validated in the MATLAB simulation. However, all the subsystems used in the simulations have been used in the experimental prototype also. The total power handled by the experimental verification system was limited to 600 W. The specifications of the various subsystems are shown in Table 11.

In the absence of the solar wind and the fuel cell sources, the battery gives back up to the DC as well as the AC loads. In the absence of the AC and DC loads

Table 11. Specifications of the subsystems.

Source	Nominal power rating
The SPV system	120 W
The wind energy system	350 W
The DC load	240 W
Three phase AC load	350 W

and if the battery is full, the power is routed back to the three-phase utility.

There could be many scenarios possible with the number of sources and loads. It is clear that any single renewable source can support the total load. The total capacity of the renewable sources including the fuel cell is 590 W. The total load to be supplied is also 590 W. In the absence of the renewable sources and the utility, the battery can support all the loads; as the battery power is routed to the AC as well as DC loads primarily through the DC bus bar. The DC bus bar voltage is 48 V. The current requirement for the total load will be

$$P = V * I;\ 590 = 48 * I. \tag{2}$$

$$I = 590/48 = 12.29A. \tag{3}$$

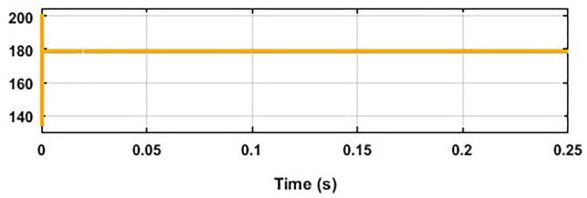

(a)

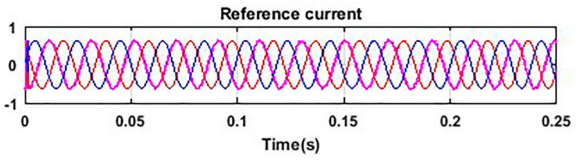

(b)

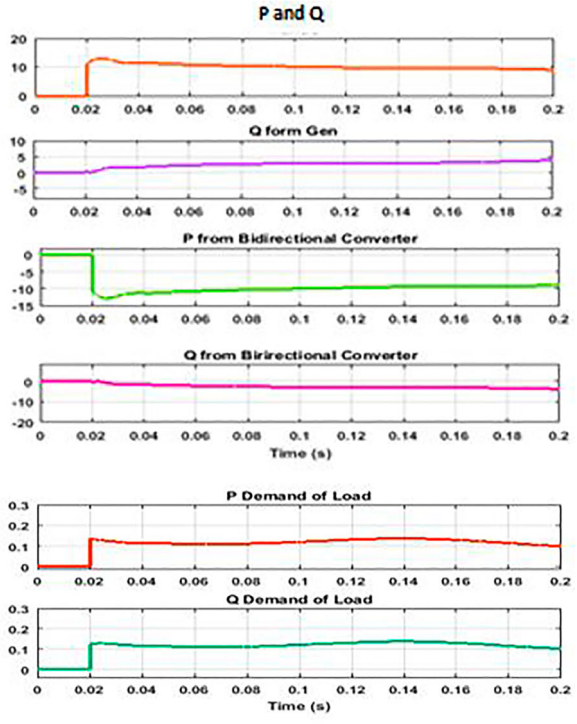

(c)

Figure 8. Power Flow Waveforms: (a) The PV voltage. (b) The Three phase reference. (c) P–Q Control schemes. (d) VI Characteristics. (e) The DC link Voltage and Current.

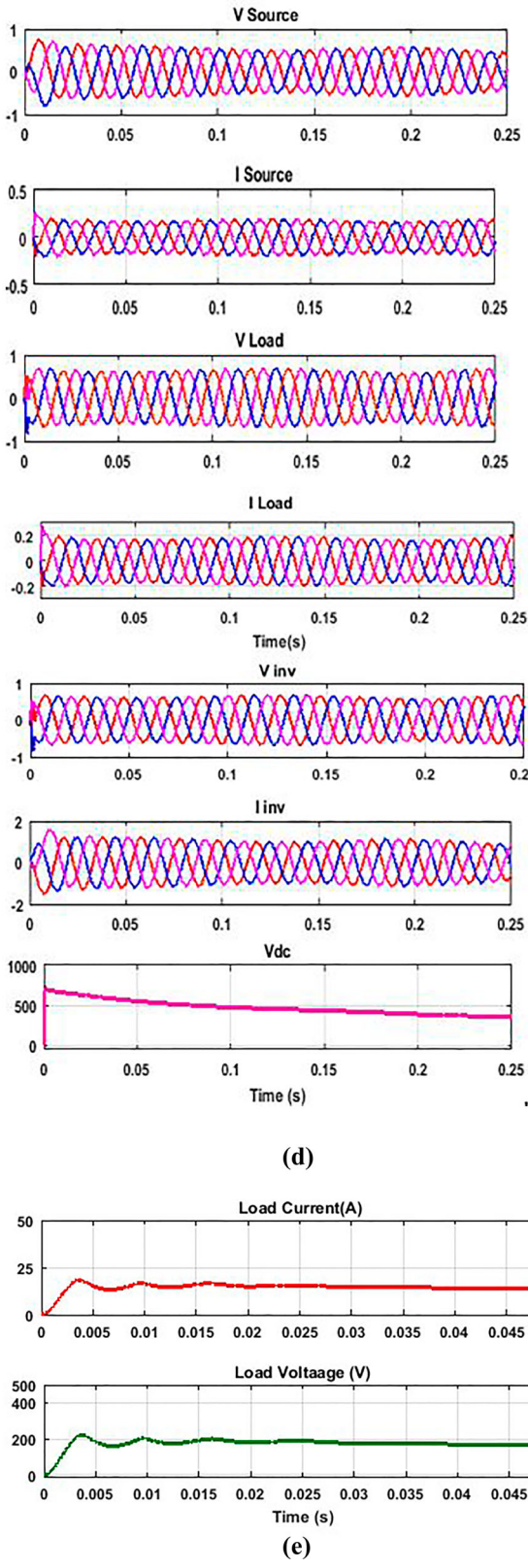

(d)

(e)

Figure 8. Continued.

For the battery to support for a total period of 12 hours, the required Ah capacity of the battery should be at least $13 * 12 = 156$ Ah. In this work, we have used a signal Lead Acid battery of nominal 12 V ratings. With terminal voltage reduced by 4 times, the Ah requirement goes high and as a result the battery of at least

Figure 9. Experimental verification setup.

Table 12. Parameters of buck boost converter.

Nominal input voltage	120 V
Output voltage	400 V
Power rating	4500 kW
Switching frequency	20 kHz
Output capacitor	2200 mF

600 Ah will be required for a full power support for 10 hours. However, in the experimental setup, the battery used is of rating 30 Ah with a nominal terminal voltage of 12 V. In between the battery and the 48 V DC bus bar is a buck and boost conversion stage. The buck converter is used to charge the battery from the DC bus bar, whereas the boost converter is used to boost the 12 V level of the battery to the required 48 V level. The buck converter is provided with the charge control feature, whereas the boost converter is equipped with the 48 V regulation systems. When the battery is in the + discharge mode even if all the renewable sources and the utility fail the battery can regulate the DC bus bar voltage at the 48 V level while the full load of 590 V is also working. When one or more renewable sources come into the microgrid and contribute power, the burden on the boost converter associated with the battery gets reduced.

4.4. Buck boost converters

All the Buck Boost converters used in this work are the generic type and they are all identical. The specifications of the components used are shown in Table 12.

4.5. Bidirectional AC/DC converter

A three-phase Graetz Bridge bi-directional power converter was used for transacting power between the DC bus bar and the AC bus bar. The circuit arrangement of the three-phase converter is shown in Figure 10.

The specifications of the components used in the bidirectional converter are shown in Table 13.

Table 13. Components of bi-directional converter.

Component	Specification
IGBT	16N60 6 Nos.
Snubber	R = 47 Ohms C = 0.1 mF
Opto coupler	MCT2E 6 Nos.
PWM	SPWM
Microcontroller	PIC 16 F877A 3 Nos.

4.6. Controls of bidirectional converter

An impo rtant novelty of the proposed system is that for the generation of sinusoidal PWM pulses, a direct microcontroller-based scheme is used without explicit carrier. It is the microcontroller that generates the PWM pulses directly. The microcontroller, using the built in ADC reads in the signal conditioned reference and the internal PWM generation unit produces the corresponding PWM. In the PIC 16F877A microcontroller, there are 8 channels of ADC and two PWM sections. The PWM sections can be initialized with the required carrier frequency. The width of the individual pulses is altered by the value of the analogue signal read by the ADC. After generating the three-phase reference signal, each of the three-phase reference signals are individually rectified and attenuated and applied to the ADC inputs A0 and A1.

A0 reads the positive half cycle. A1 reads the polarity changed negative half cycle. The two PWM outputs are applied to the complementary switches in each leg. A Zero Crossing Detector (ZCD) is also used so that the upper or the lower switch in each leg can be selected based on the zero-crossing timing. Three microcontrollers are used for the three phases. The signals corresponding to this section are shown in Figures 11 and 12.

As far the control schemes are concerned, the bidirectional converter ensures that the voltage across the DC bus and that across the AC bus are maintained at the desired level. The AC and the DC voltages are monitored and signal conditioned and read by the ADC section of the local microcontroller. PI controllers are embedded in the local controller and the control systems alter the three-phase reference such that the DC link voltage and the AC voltage at the point of common coupling are maintained.

For the regulation of the voltage at the point of common coupling, the modulation index is used. For the regulation of the DC link voltage, the phase angle of the reference signal is altered by the shifting operation carried out in the data used for the PWM. The power balance study for the experimental verification system has been done for three scenarios. For the experimental verification, the wind energy source was replaced by a DC power source derived through a DBR drawing power from the utility.

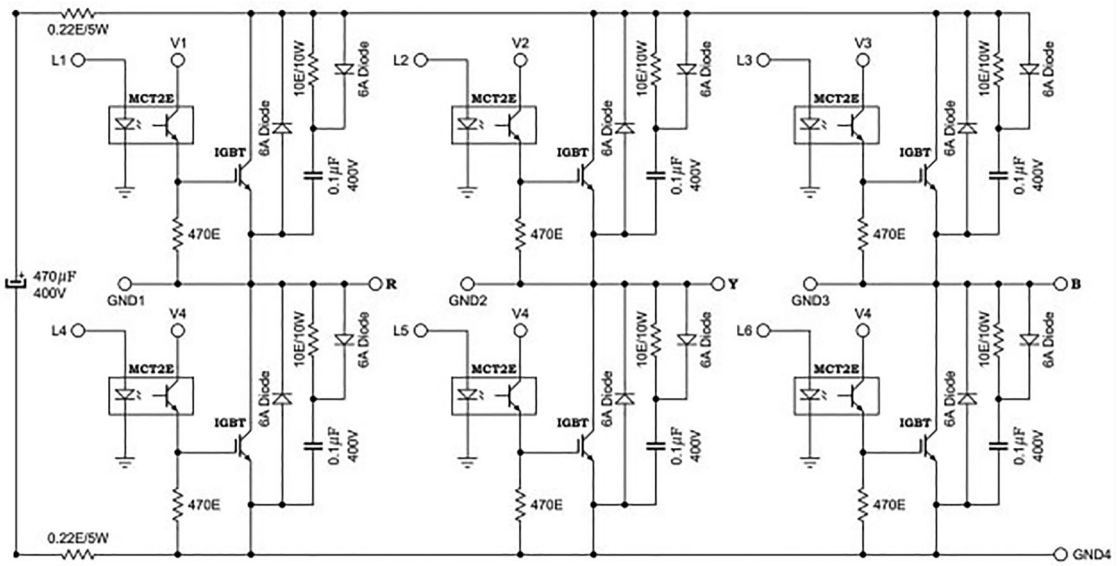

Figure 10. Circuit diagram of the three phase converter.

Table 14. Power balance requirement 1.

Source/Load	Power supplied/Drawn
Wind source	320 W
Solar PV source	108 W
Total energy source	428 W
DC load	240 W
AC load	120 W
Power to battery	68 W

Table 15. Power balance requirement 2.

Source/Load	Power supplied/Drawn
Wind source	0 W
Solar PV source	110 W
Total energy source	110 W
DC load	240 W
AC load	120 W
Power to battery	0 W
Power drawn from utility	250 W

4.6.1. Scenario 1

With the wind and the PV source available, the total renewable energy generated and the loads are shown in Table 14.

4.6.2. Scenario 2

With the wind source not active and the PV source available, the total renewable energy generated are shown in Table 15.

4.6.3. Scenario 3

With the utility, wind and the PV sources unavailable, the only load to be served was the critical load and this load was met by the battery. The power balance is shown in Table 16.

The basic power balance requirement can be met only if the voltages across the AC bus bar and the DC bus bars are maintained. The controllers associated with the bidirectional converter takes care of the DC link voltage as well as the AC bus bar voltage. Figure 11(a) shows the DC link voltage when the renewable energy sources are available. In this case, the DC link is quite free from ripple.

Table 16. Power balance requirement 3.

Source/Load	Power supplied/Drawn
Wind source	0 W
Solar PV source	0 W
Total energy source	0 W
DC load	60 W
AC load	0 W
Power from battery	68 W

With the renewable energy sources absent, the DC bus bar is maintained from the power drawn from the AC utility source and the DC in this case shows some ripple as shown in Figure 11(a,b).

One of the major contributions of the work is that the sinusoidal PWM is implemented directly by the embedded system and not by an explicit carrier AD (Analogue Device) comparator. The ADC section and the PWM section of the PIC microcontroller generates the SPWM (Sinusoidal pulse width modulation) pulses directly and the switching pulses generated for the three-phase bidirectional converter is shown in Figure 11(c).

The AC bus bar output for one of the three phases is shown in Figure 11(d). The FFT (Fast Fourier transform) of the AC phase voltage is also shown in Figure 11(d).

With the sudden inclusion of additional DC load, the DC link voltage falls. Also, with the sudden removal or absence of the renewable sources, the DC link voltage falls. However, by the action of the bidirectional converter, the DC link voltage is restored. The fall and restoration of the DC link voltage for **t**he two cases were recorded and are shown in Figure 12(a). ZCD is used for

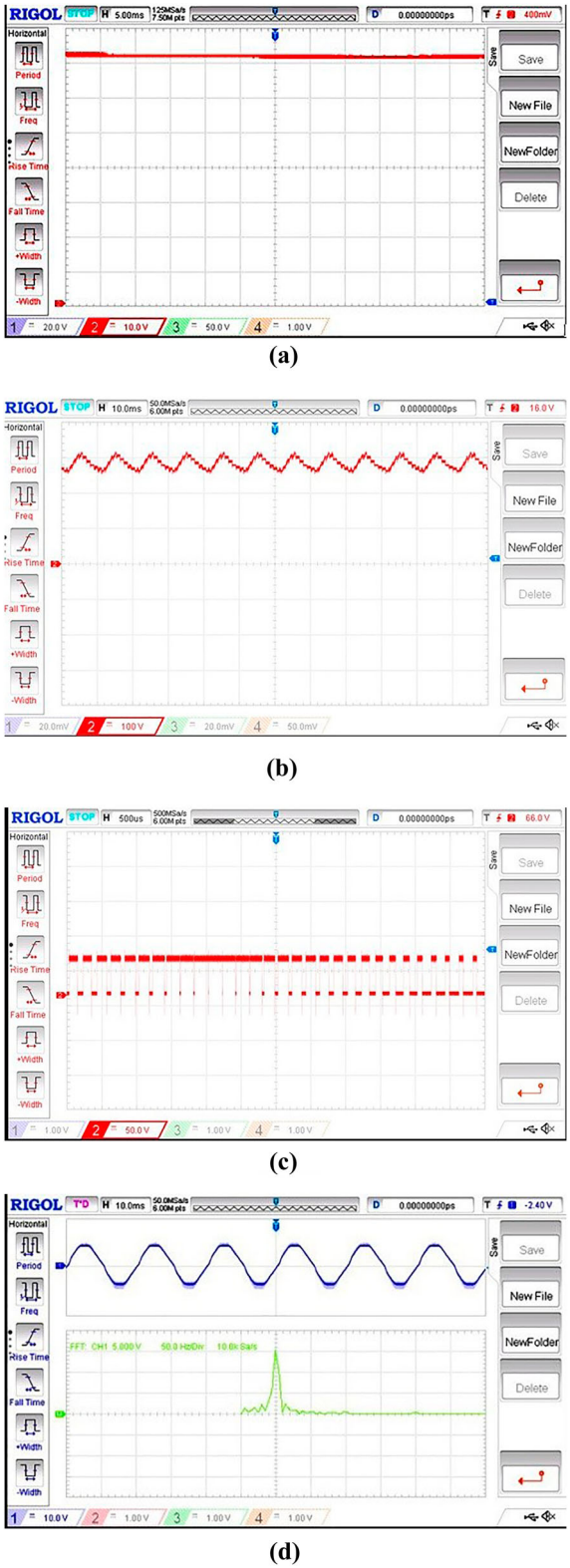

Figure 11. (a) DC Bus bar Voltage. (b) Ripple in DC link Voltage. (c) Switching Pulses (SPWM). (d) Phase voltage and FFT of AC Bus. (a), (b) (d) X axis Time 1 cm = 10 milli second; y axis 1 cm = 20 V; Figure 11 (b) uses 1:10external attenuator. Figure 11. (c) 1 cm = 5 V Figure 11 (c). X Axis 1 cm = 20 micro seconds.

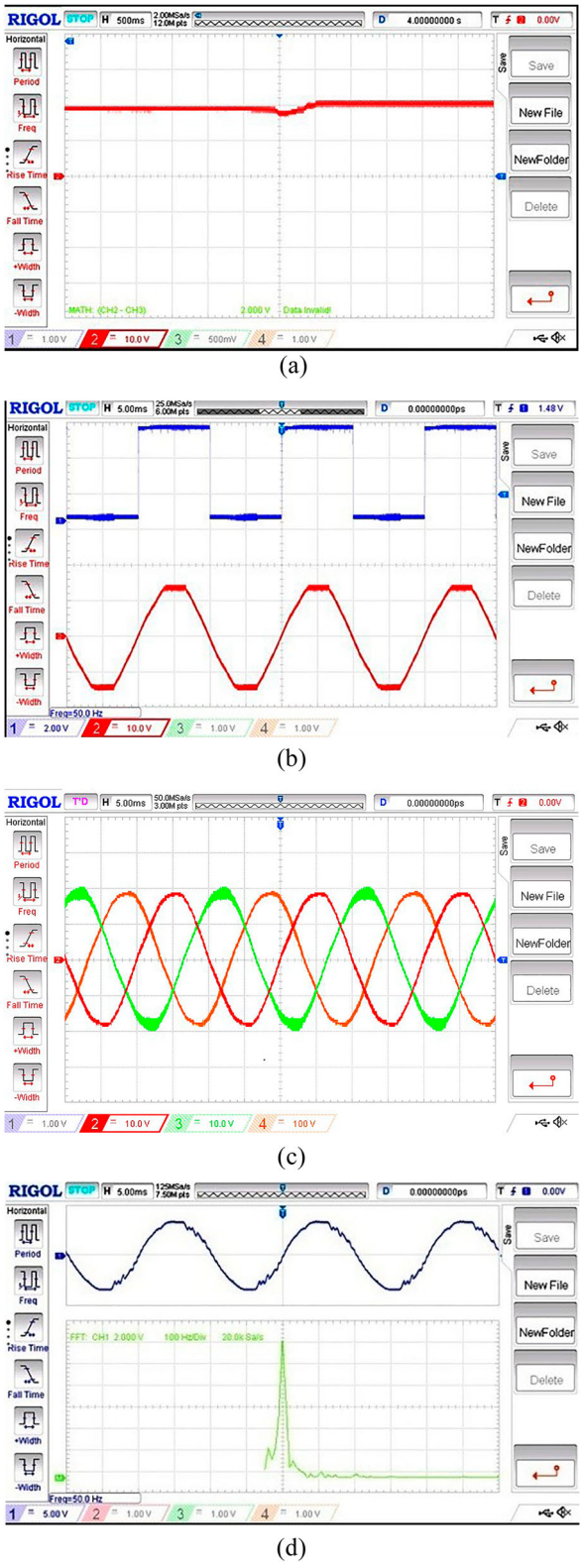

Figure 12. Important experimental waveforms. (a) DC link voltage subjected to Source voltage disturbance. x axis time 1 cm = 10 ms; y axis (1 cm = 200 V). (b) Zero-Crossing detection signals x axis 1 cm = 5 milli seconds; y axis 1 cm = 2Volts. (c). Three phase AC voltage x axis 1 cm = 5 ms y axis 1 cm = 100 Volts. (d) R phase voltage and FFT plot. x axis 1 cm = 5 milli seconds, y axis 1 cm = 5 volts (40:1 External Attenuation).

this purpose. The waveform pertaining to the reference signal and the ZCD are shown in Figure 12(b).

When the utility source is absent and the renewable energy sources are sufficiently available, the bidirectional converter feeds the AC load through the AC bus bar. However, since in this case the sole AC power supply is from the bidirectional converter, the

AC voltages of the three phases containing harmonics are shown in Figure 12(c). With more load on the AC bus bar, the AC waveform degrades and the resulting waveform is shown in Figure 12(d).

The special features and novelties adopted and achieved in this work can be consolidated as follows.

a. The power flow is maintained by the voltage balance techniques adopted on the AC and DC bus bars using the P–Q theory.
b. The complete hardware relied upon digital or embedded systems. This includes the SPWM pulse generation as well.
c. There is a central supervisory system operated through the GUI contained in the master control PC. Power transactions in real time could be recorded as well.
d. Overriding feature was also included since the master control unit can directly include or exclude any source or load.
e. The Sliding Mode Controller MPPT is used for the solar and wind energy sources. This was tested in simulation for both wind and solar PV systems in the simulation platform. In the case of hardware, only the PV system was equipped with the SMC as it was only a representative DC source used in place of the Wind Energy Subsystem.

5. Conclusion

A novel system of management of the microgrid using the SCADA system has been proposed and validated in this work. Both simulations and experimental verifications have been carried out. The proposed idea uses wired data collection between the local nodes and the master controller. It has been established that the proposed system monitors the variations that happen in environmental conditions that influence the generation of power. The master controller also monitors the power flowing into the load and issues necessary commands such that in the sources and the loads an efficient power transaction is carried out. Essentially the work suggests the use of local controllers for local voltage regulation and MPPT activities, whereas the master controller should take care of inter-converter power transactions.

Acknowledgements

The authors are highly grateful to the Director General **Dr.K. Balaraman**, **Dr. Rajesh Katyal** Deputy Director General & Division Head, **David Solomon.J.C** Director & Division Head **NIWE (National Institute of Wind Energy)** for giving me permission to use the Research Data's and Information's on this work.

Disclosure statement

No potential conflict of interest was reported by the author(s).

Funding

This work was supported by the University Grants Commission: [Grant Number F1-17.1/2017-18/RGNF-2017-18-SC-TAM-32683].

ORCID

T. Srikanth http://orcid.org/0000-0002-5330-5989

References

[1] Zhang Y, Xiang Y, Wang L. Power system reliability assessment incorporating cyber attacks against wind farm energy management systems. IEEE Trans Smart Grid. 2017;8m(5):2343–2357.
[2] Wang Y, Xu W, Shen J. Online tracking of transmission-line parameters using SCADA data. IEEE Trans Power Delivery. 2016;31(2):674–682.
[3] Salgado AR, Esquivel CRF, Guizar JGC. SCADA and PMU measurements for improving power system state estimation. IEEE Latin Am Trans. 2015;13(7):2245–2251.
[4] Soonee SK, Agrawal VK, Agarwal PK, et al. The view from the wide side: wide-area monitoring systems in India. IEEE Power Energ Mag. 2015;13(5):49–59.
[5] Grilo AM, Chen J, Díaz M, et al. An integrated WSAN and SCADA system for monitoring a critical infrastructure. IEEE Trans Ind Inf. 2014;10(3):1755–1764.
[6] Taylor Z, Akhavan-Hejazi H, Cortez E, et al. Customer-side SCADA assisted large battery operation optimization for distribution feeder peak load shaving. IEEE Trans Smart Grid. 2019;10(1):992–1004.
[7] Schossig T, Klien A, Steinhauser F. Methods for testing automation and control. J Eng. 2018;2018(15):1340–1343.
[8] Pandit RK, Infield D. SCADA-based wind turbine anomaly detection using Gaussian process models for wind turbine condition monitoring purposes. IET Renew Power Gener. 2018;12(11):249–1255.
[9] Kong X, Yan Z, Guo R, et al. Three-stage distributed state estimation for AC-DC hybrid distribution network under mixed measurement environment. IEEE Access. 2018;6:39027–39036.
[10] Al Badwawi R, Issa WR, Mallick TK, et al. Controller. Energy. 2019;10(1):94–104.
[11] Kharraz A, Mishra Y, Sree ram V. Discrete-event systems supervisory control for a custom power park. IEEE Trans Smart Grid. 2019;10(1):483–492.
[12] Hou X, Sun Y, Lu J, et al. Distributed hierarchical control of AC microgrid operating in grid-connected, islanded and their transition modes. IEEE Access. 2018;6:77388–77401.
[13] Guarnieri M, Bovo A, Giovannelli A, et al. A real multi technology microgrid in venice: a design review. IEEE Ind Electron Mag. 2018;12(3):19–31.
[14] Busarello TDC, Mortezae A, Péres A, et al. Application of the conservative power theory current decomposition in a load power-sharing strategy among distributed energy resources. IEEE Trans Ind Appl. 2018;54(4):3771–3781.
[15] Bhattacharjee C, Roy BK. Fuzzy-supervisory control of a hybrid system to improve contractual grid support with fuzzy proportional–derivative and integral control for power quality improvement. IET Gener Trans Distrib. 2018;12(7):1455–1465.

[16] Knudsen J, Bendtsen JD, Andersen P, et al. Supervisory control implementation on diesel-driven generator sets. IEEE Trans Ind Electron. 2018;65(12):9698–9705.
[17] Sowmmiya U, Govindarajan U. Control and power transfer operation of WRIG-based WECS in a hybrid AC/DC microgrid. IET Renew Power Gener. 2018;12 (3):359–373.
[18] Sharma RK, Mishra S. Dynamic power management and control of a PV PEM fuel-cell-based standalone AC/DC microgrid using hybrid energy storage. IEEE Trans Ind Appl. 2018;54(1):526–538.
[19] Ko H-S, Ryu K-S, Kim DJ, et al. Supervisory power quality control scheme for a grid-off microgrid. IEEE Trans Sustain Energy. 2018;9 (3):1003–1010.
[20] Sun L, Wu G, Xue Y, et al. Coordinated control strategies for fuel cell power plant in a microgrid. IEEE Trans Energy Convers. 2018;33(1):1–9.
[21] Allam MA, Hamad AA, Kazerani M, et al. A novel dynamic power routing scheme to maximize loadability of islanded hybrid AC/DC microgrids under unbalanced AC loading. IEEE Trans Smart Grid. 2018;9(6):5798–5809.
[22] Alvarez-Herault MC, Labonne A, Touré S, et al. An original smart-grids test bed to teach feeder automation functions in a distribution grid. IEEE Trans Power Syst. 2018;33(1):373–385.
[23] Pashajavid E, Ghosh A, Zare F. A multimode supervisory control scheme for coupling remote droop-regulated microgrids. IEEE Trans Smart Grid. 2018;9 (5):5381–5392.
[24] Hosseinzadeh M, Salmasi FR. Fault-tolerant supervisory controller for a hybrid AC/DC micro-grid. IEEE Trans Smart Grid. 2018;9(4):2809–2823.